ORO 5126-35

EMPIRICAL LIMITATIONS OF ENERGY DISSIPATION IN ^{252}Cf(sf)

H. Schultheis and R. Schultheis
Department of Physics and Astronomy
University of Maryland, College Park, Maryland 20742 U.S.A.

and

Institut für Theoretische Physik
Universität Tübingen, D-7400 Tübingen, West Germany

April 1978

U. of Md. TR #78-058
U. of Md. PP #78-141

UNIVERSITY OF MARYLAND
DEPARTMENT OF PHYSICS AND ASTRONOMY
COLLEGE PARK, MARYLAND

DISCLAIMER

ORO 5126-35
U. of Md. TR #78-058
U. of Md. PP #78-141

EMPIRICAL LIMITATIONS OF ENERGY DISSIPATION IN ^{252}Cf(sf) †

H. Schultheis and R. Schultheis
Department of Physics and Astronomy
University of Maryland, College Park, Maryland 20742 U.S.A.
and
Institut für Theoretische Physik
Universität Tübingen, D-7400 Tübingen, West Germany

April 1978

ABSTRACT

Limitations for the energy dissipated in the spontaneous fission of ^{252}Cf have been studied on the basis of the experimental fragment kinetic energies, neutron and γ data and the calculated (static) potential energies of the fragments. Upper bounds for the dissipated energy are obtained by restricting the parameter space of the fissioning system to the domain which is compatible with the experimental post-scission data, and by computing the maximum energy available in this domain for dissipation. No assumptions have been made about the fission dynamics or the dissipation mechanism. A numerical evaluation has been performed for 19 pairs of fragments in ^{252}Cf(sf), taking into account spheroidal fragment shapes with diffuse surface, nuclear interaction and Coulomb excitation effects. The energy available for internal excitation at scission is found to be small (≤ 10 MeV). An analysis of the uncertainties entering into this result shows that high dissipation in ^{252}Cf(sf) is incompatible with the existing experimental data unless peculiar fragment shapes are assumed. Upper bounds are also given for the fragment deformations. We discuss the hypothesis of minimum potential energy at scission, the influence of fragment shell effects, and the relevance of data from ternary fission.

KEYWORD ABSTRACT

[RADIOACTIVITY, FISSION ^{252}Cf(sf); calculated energy dissipation, fragment deformation.]

I. INTRODUCTION

The problem of energy dissipation is crucial for the conventional treatment of fission in heavy nuclei. Apart from few exceptions (e.g., Hill and Wheeler[1]), the time evolution of the system is studied as a function of a small number of parameters, that account for the few "important" collective degrees of freedom. This treatment corresponds to the experimental situation, as only certain collective properties of the compound nucleus and its fragments are accessible to measurements. As the conservation of energy does not apply to such a reasonable, but arbitrary, selection of degrees of freedom, the problem of energy dissipation into the other (intrinsic) degrees of freedom must be overcome.

Contradictory assumptions have been made earlier about this crucial effect ranging from zero-dissipation[1-5] to almost complete damping.[6] In particular the contribution of one-body and two-body effects to the dissipation mechanism is controversial.[7-13] Until today the strength of the dissipation and the magnitude of the internal excitation energy resulting from it are still unknown. A number of estimates has been given for the internal excitation energy in certain fission reactions. They are based on experimental information,[7,14-20] on hydrodynamical calculations with adjustable viscosity,[7-10] on particular microscopic models,[13,21-23] or on combinations of several approaches.[18,24,25] The estimated internal excitation energies derived from theoretical models generally are very large (some are even larger than the available energy at scission). The estimates based on experimental data usually yield smaller values. Some of them, however, neglect certain types of excitation or make use of crude approximations for the nuclear shape or the potential energy.

It is the aim of the present paper to determine energy dissipation limitations in the spontaneous fission of ^{252}Cf. In order to arrive at as firm a determination as possible we rely only on quantities which are known with relatively high accuracy, namely the calculated fragment deformation energies, the Coulomb and nuclear interaction energies between them, and experimental post-scission data. In particular we avoid any models or assumptions for the dynamics of the nuclear motion or the mechanism of dissipation in fission. This is achieved by numerically scanning the space of deformation parameters of each pair of fragments at a given fragment separation. At each step we determine (within certain bounds) the kinetic and excitation energies the fragments would have at infinite separation, and compare these values with the corresponding experimental data. Then the maximum energy available for dissipation and collective vibration is numerically searched for under the constraint that the nuclear deformation be compatible with the experimental post-scission data.

The method of the present paper differs from our previous estimate[18] in the assumption of diffuse nuclear surfaces. This requires to abandon the concept of a scission "point" (with a discontinuous break-up of a sharp-surface droplet into fragments with square-well density distributions). Instead, a sequence of fragment separations with decreasing neck density is considered (cf. Sect. III). In addition, the nuclear interaction energy between the fragments is now taken into account. The post-scission Coulomb excitation is no longer assumed to be small. It is treated as a variational parameter that may assume arbitrary values (up to the experimental fragment excitation energy). Furthermore we have abandoned our previous restriction that the upper bound of the dissipated (plus non-translational collective) energy be

a constant fraction of the measured fragment excitation energy, independent of the mass asymmetry of the fragmentation. The new results show that this assumption is in fact not well fulfilled, the resulting dissipation bound, however, is of the same order.

In Subsect. II.A several limiting conditions are derived for fragment deformations and energy dissipation in fission. These are valid for arbitrary nuclear deformations. The limitations are evaluated assuming spheroidal fragments (as described in Subsect. II.B) for the spontaneous fission of ^{252}Cf where particularly accurate experimental data are available (Subsect. II.C). The relaxation of the assumptions of Ref. 18 and a thorough examination of the accuracy of the results (Subsect. III.B) leads to a number of new findings concerning the fragment shapes (Subsect. III.C) the minimum potential energy hypothesis (Subsect. III.D) and the relevancy of ternary fission data for binary fission results (Subsect. III.E). The conclusions are summarized in Sect. IV.

II. METHOD

The method described in the following subsection does not require any assumption about the shape of the fissioning nucleus or about the functional form of its potential energy. Therefore, the relations of Subsect. II.A are derived for an arbitrary set of shape parameters α. For the numerical evaluation of ^{252}Cf(sf), however, we make use of the conventional spheroidal approximation for the fragment shapes. This is described in Subsect. II.B.

A. Energy Available for Dissipation

We consider the spontaneous fission of the parent nucleus (Z_0,A_0) into two fragments with given mass and charge numbers (Z_1,A_1) and (Z_2,A_2). The

energy release of that reaction experimentally shows up as fragment kinetic energy $E^{kin}_{expt}(Z_1,A_1,Z_2,A_2)$, neutron and γ-ray energies. On the other hand, the energy release is equal to the difference of the ground-state potential energy V of the parent nucleus and that of the fragments (if we neglect the small change in zero-point energy), i.e.,

$$V(Z_0,A_0,\alpha_0^{gst}) - \sum_{i=1}^{2} V(Z_i,A_i,\alpha_i^{gst}) = \sum_{i=1}^{2} E^{*}_{expt}(Z_i,A_i) + E^{kin}_{expt}(Z_1,A_1,Z_2,A_2). \tag{2.1}$$

Here α_0, α_1, and α_2 denote arbitrary sets of deformation parameters of the parent nucleus (i = 0) and the fragments (i = 1,2). The superscript gst refers to the gound-state deformation. The total energy of neutron and γ-quanta emitted from fragment (i) is denoted by $E^{*}_{expt}(Z_i,A_i)$. From the experimental quantities E^{*}_{expt} and E^{kin}_{expt} only the mean values for each fragmentation enter into the evaluation (cf. Subsect. II.C). A possibly ambiguous division of the experimental excitation energy between heavy and light fragments (e.g., due to scission neutrons) does not affect the present analysis as will be discussed below.

Any excitation during the descent from saddle to scission is either collective (related to changes in the collective coordinates α_0) or internal (related to other degrees of freedom). At scission they result in translational collective energy E_{trans} (corresponding to non-zero relative velocity between the centers of mass of both fragments) and other (vibrational or rotational) collective or internal excitation energy X. The total amount of excitation energy E_{trans} + X at a certain deformation α_0 equals the decrease in potential energy relative to the ground state of the parent nucleus, i.e.,

$$X + E_{trans} = V(Z_0,A_0,\alpha_0^{gst}) - V(Z_0,A_0,\alpha_0). \tag{2.2}$$

It is convenient to define the interaction energy V_{int} (due to Coulomb and nuclear forces) between two arbitrary parts (i = 1,2) of the system as

$$V_{int}(Z_1,A_1,Z_2,A_2,\alpha_0,\alpha_1,\alpha_2) = V(Z_0,A_0,\alpha_0) - \sum_{i=1}^{2} V(Z_i,A_i,\alpha_i). \tag{2.3}$$

It follows then from Eqs. (2.1) - (2.3) that

$$X + E_{trans} = \sum_{i=1}^{2} [E^{*}_{expt}(Z_i,A_i) + V(Z_i,A_i,\alpha_i^{gst}) - V(Z_i,A_i,\alpha_i)]$$

$$- V_{int}(Z_1,A_1,Z_2,A_2,\alpha_0,\alpha_1,\alpha_2) + E^{kin}_{expt}(Z_1,A_1,Z_2,A_2). \quad (2.4)$$

The final fragment kinetic energy E^{kin}_{expt} is almost equal to the sum of pre-scission kinetic energy E_{trans} and the interaction energy V_{int} at scission. It may be reduced by a certain amount δ (e.g., due to post-scission Coulomb excitation in the strongly non-central Coulomb field of the deformed fragments). Therefore,

$$E^{kin}_{expt}(Z_1,A_1,Z_2,A_2) = E_{trans} + V_{int}(Z_1,A_1,Z_2,A_2,\alpha_0,\alpha_1,\alpha_2) - \delta \quad (2.5)$$

and, according to Eq. (2.4)

$$X = \sum_{i=1}^{2} [E^{*}_{expt}(Z_i,A_i) + V(Z_i,A_i,\alpha_i^{gst}) - V(Z_i,A_i,\alpha_i)] - \delta. \quad (2.6)$$

Equations (2.5) and (2.6) are coupled, because V_{int} and $V(Z_i,A_i,\alpha_i)$ are (numerically) given functions of the same sets of variables, α_1 and α_2. In order to determine an upper bound for both the dissipated energy and the non-translational collective excitation energy, we eliminate the unknown quantity E_{trans} in Eq. (2.5) by introducing the inequality

$$E^{kin}_{expt}(Z_1,A_1,Z_2,A_2) \geq V_{int}(Z_1,A_1,Z_2,A_2,\alpha_0,\alpha_1,\alpha_2) - \delta \quad (2.7)$$

and treat δ as a numerical parameter

$$0 \leq \delta \leq \sum_{i=1}^{2} E^{*}_{expt}(Z_i,A_i). \quad (2.8)$$

Then for each fragment pair (Z_1,A_1) and (Z_2,A_2) an upper bound X_{max} can be determined by maximizing the right-hand side of Eq. (2.6) under the constraints (2.7) and (2.8). Since $E^{*}_{expt}(Z_i,A_i)$ and $V(Z_i,A_i,\alpha_i^{gst})$ are constants this amounts to numerically searching for the constraint minimum of $V(Z_1,A_1,\alpha_1) + V(Z_2,A_2,\alpha_2) + \delta$ as a function of the sets of deformation parameters α_1 and α_2 of the fragments and an additional parameter δ. This has been performed for ^{252}Cf(sf) making use of the shape parametrization, potential energy and experimental data, that are described in the following subsections. It turned

out that the dependence of X_{max} on the parameter δ and on the distribution of $X = X(H) + X(L)$ between heavy and light fragment is very weak. In practice the values of X_{max} obtained for $\delta = 0$ and $X(H)/X(L) = E^{*}_{expt}(H)/E^{*}_{expt}(L)$ were found to approximate the general result with sufficient accuracy.

From Eq. (2.6) also follows that

$$\sum_{i=1}^{2} V(Z_i,A_i,\alpha_i) \leq \sum_{i=1}^{2} [E^{*}_{expt}(Z_i,A_i) + V(Z_i,A_i,\alpha_i^{gst})]. \quad (2.9)$$

The inequality (2.9) will be used in Subsect. III.C in order to obtain upper limits for the fragment deformations.

Figure 1 illustrates the method for a one-dimensional parameter space (e.g., symmetric fission with spheroidal fragment deformation $\alpha_1 = \alpha_2 = \beta$. Here $\delta = 0$ and zero nuclear interaction is assumed for simplicity. The Coulomb repulsion, V_{int}, between the fragments is a decreasing function of β. Therefore, the constraint (2.7) is fulfilled only if $\beta \geq \beta_{min}$ in Fig. 1b. Under this constraint the deformation energy of Fig. 1a has a minimum at $\beta = \beta_{min}$ and the maximum energy available for (rotational, vibrational and internal) excitation is given by X_{max}. In Fig. 1a the upper limit β_{max} of the fragment deformation is also given as required by inequality (2.9). In the general case of asymmetric fission (with nuclear interaction and $\delta \neq 0$) the computation is complicated because at least two interdependent parameters $\beta_{min}(1)$ and $\beta_{min}(2)$ replace the single value β_{min} and the functions $V(\beta)$ and $V_{int}(\beta)$ may not be monotonic in the constrained parameter space.

B. Potential Energy

For the evaluation of Eqs. (2.6) - (2.9) we parametrize the shape of the fissioning nucleus by two coaxial spheroids. Such a spheroidal parametrization has often been used for the potential energy at scission and after scission.[2,3,18,26-36] As only energy *differences* between such configurations enter into our calculation the spheroidal approximation should be sufficient. Higher axial[21,37-39] or non-axial[35] deformations could in principle be included,

but this would require much more computer time. Moreover, the spheroical approximation enables the study of inhomogeneities in the charge and mass distributions at the nuclear surface, because the effect of the diffuse surface on the energy can be treated by corrections with high accuracy.

We consider for the radial fragment density a Fermi distribution with constant surface thickness. Then the shape of the nucleus is specified by the distance d between the equivalent sharp density surfaces of the fragments, and the Bohr-Mottelson[39] parameters β_i (i = 1,2) for the fragment deformations. The semi-axes x_i, y_i and z_i are then given by

$$x_i = y_i = R(\beta_i,A_i)[1 - \tfrac{1}{2}(\tfrac{5}{4\pi})^{1/2}\beta_i] \tag{2.10}$$

$$z_i = R(\beta_i,A_i)[1 + (\tfrac{5}{4\pi})^{1/2}\beta_i] \tag{2.11}$$

where

$$R(\beta_i,A_i) = r_c A_i^{1/3}[1 - \tfrac{15}{16\pi}\beta_i^2 + \tfrac{1}{4}(\tfrac{5}{4\pi})^{3/2}\beta_i^3]^{-1/3} \tag{2.12}$$

is the volume conservation condition if

$$\sum_{i=1}^{2} A_i = A_0 \tag{2.13}$$

for each fragment pair. The liquid-drop radius parameter r_c is given below.

The potential energy V consists of the liquid-drop (LDM) and shell energy of each fragment, and a nuclear interaction (NI) and Coulomb repulsion (CR) energy between them:

$$V(Z_1,Z_2,A_1,A_2,\beta_1,\beta_2,d) = \sum_{i=1}^{2}[V_{LDM}(Z_i,A_i,\beta_i) + V_{shell}(Z_i,A_i,\beta_i)] + V_{CR}(Z_1,Z_2,A_1,A_2,\beta_1,\beta_2,d) + V_{NI}(Z_0,A_1,A_2,\beta_1,\beta_2,d). \tag{2.14}$$

The liquid-drop energy V_{LDM} is calculated after Myers and Swiatecki[40,41] with explicit expressions for the area of the equivalent sharp density surface

|S| and for the Coulomb energy[42] of the (homogeneous) charge Ze, i.e.,

$$V_{LDM}(Z,A,\beta) = a_2[1 - \kappa(\tfrac{N-Z}{A})^2]\frac{|S|}{4\pi r_c^2} + \frac{3}{10}\frac{Z^2e^2}{r_c A^{1/3}}\frac{(1-\varepsilon^2)^{1/3}}{\varepsilon}\ln\frac{1+\varepsilon}{1-\varepsilon} + V_{CS} \tag{2.15}$$

where

$$|S| = 2\pi x\{x + \frac{z^2}{\sqrt{z^2-x^2}}\arcsin\frac{\sqrt{z^2-x^2}}{z}\} \tag{2.16}$$

and

$$\varepsilon^2 = 1 - (x/z)^2 \qquad (z > x) \tag{2.17}$$

are functions of the semi-axes x and z. The parameters a_2, κ, and r_c are given below. The inhomogeneity of the charge distribution at the surface can be taken into account by a correction[40] V_{CS} which is independent of shape in high order.[40,43] Here, it need not be considered explicitly because it cancels in Eq. (2.6). The influence of the diffuse fragment surfaces on the nuclear interaction is treated in Eq. (2.27).

The shell correction V_{shell} is taken to be that of Myers and Swiatecki.[40,41] We prefer this over Strutinsky-type shell corrections for several reasons. First, its uncomplicated functional form enables the rapid computation of a large number of fragment deformations, which is necessary for the minimization procedure for Eq. (2.6). Second, it turns out that secondary minima of the fragments (at $\beta_i > \beta_i^{gst}$) have almost no influence on the results (cf. Sect. III). Third, the Myers-Swiatecki shell energy is expected to describe the potential energy of fragments far off the line of β-stability with sufficient accuracy, as it accounts well for the binding energies and quadrupole moments of a large number of nuclei throughout the periodic table. A comparison with other shell corrections will be given in Sect. III.

The shell correction of Myers and Swiatecki[40,41] reads

$$V_{shell}(Z,A,\beta) = C[\frac{F(N)+F(Z)}{(A/2)^{2/3}} - cA^{1/3}](1-2\theta^2)\exp(-\theta^2) \quad (2.18)$$

where

$$F(m) = \frac{3}{5}\frac{M_i^{5/3}-M_{i-1}^{5/3}}{M_i - M_{i-1}}(m-M_{i-1}) - \frac{3}{5}(m^{5/3}-M_{i-1}^{5/3}) \quad (2.19)$$

and M_i and M_{i-1} denote the nearest (spherical) magic numbers[40]

$$M_{i-1} \le m \le M_i. \quad (2.20)$$

For spheroids θ in Eq. (2.18) is related to the Hill-Wheeler parameter[1,40,44] σ by

$$\theta^2 = \frac{(r_c A^{1/3})^2 \frac{1}{5}\sigma^2(1-\frac{1}{7}\sigma)}{a^2} \quad (2.21)$$

and to the major semi-axis z by

$$\sigma = \ln(\frac{z}{r_c A^{1/3}}). \quad (2.22)$$

The parameters C, c, a and r_c are given below.

The Coulomb repulsion between the two fragments is calculated according to Nix[2]

$$V_{CR}(Z_1,Z_2,A_1,A_2,\beta_1,\beta_2,d) = \frac{Z_1 Z_2 e^2}{z_1+z_2+d}[s(\lambda_1)+s(\lambda_2)-1+S(\lambda_1,\lambda_2)] \quad (2.23)$$

with

$$\lambda_i^2 = \frac{z_i^2 - x_i^2}{(z_1+z_2+d)^2} \quad (2.24)$$

and

$$S(\lambda_1,\lambda_2) = \sum_{j=1}^{\infty}\sum_{k=1}^{\infty}\frac{3}{(2j+1)(2j+3)}\frac{3}{(2k+1)(2k+3)}\frac{(2j+2k)!}{(2j)!(2k)!}\lambda_1^{2j}\lambda_2^{2k} \quad (2.25)$$

and

$$s(\lambda_i) = \frac{3}{4}(\frac{1}{\lambda_i} - \frac{1}{\lambda_i^3})\ln\frac{1+\lambda_i}{1-\lambda_i} + \frac{3}{2}\frac{1}{\lambda_i^2}. \quad (2.26)$$

As has been pointed out in Ref. 45, the effect of the diffuse surface on the Coulomb repulsion between the fragments is contained in the term V_{NI}.

For the nuclear interaction energy we have taken that of Krappe and Nix[46] (slightly modified by introducing the mean radii of curvature r_i of the equivalent sharp density surfaces at the tips of the spheroidal fragments),

$$V_{NI}(Z_0,A_1,A_2,\beta_1,\beta_2,d) = -4(a_0/r_0)^2 a_s[1-\kappa_s(\frac{N_0-Z_0}{A_0})^2] \cdot g(r_1/a_0)g(r_2/a_0)\exp(-\frac{r_1+r_2+d}{a_0})(\frac{r_1+r_2+d}{a_0})^{-1} \quad (2.27)$$

with

$$r_i = r_c^3 A_i/z_i^2 \quad (2.28)$$

and

$$g(x) = x\cosh x - \sinh x. \quad (2.29)$$

For comparison, we have also used the nuclear interaction energy of Bass[47] (with a Woods-Saxon form factor constant of 0.7 fm[48,49]); it turned out that our results are not very sensitive to the particular form of V_{NI} (cf. Sect. III).

Ten parameters enter into the calculation of the potential energy. The liquid-drop energy V_{LDM} contains the parameters[41]

$$a_2 = 17.9439 \text{ MeV} \quad (2.30a)$$

$$\kappa = 1.7826 \quad (2.30b)$$

$$r_c = 1.2249 \text{ fm}. \quad (2.30c)$$

The parameters of the shell correction V_{shell} are[41]

$$C = 5.8 \text{ MeV} \quad (2.31a)$$

$$c = 0.325 \quad (2.31b)$$

$$a = 0.444\ r_c. \quad (2.31c)$$

The nuclear interaction energy V_{NI} depends on four parameters

$$r_0 = 1.16 \text{ fm} \tag{2.32a}$$

$$a_0 = 1.4 \text{ fm} \tag{2.32b}$$

$$a_s = 24.7 \text{ MeV} \tag{2.32c}$$

$$\kappa_s = 4.0. \tag{2.32d}$$

Even if the physical meaning of some of the parameters (2.32) coincides with (2.30), the fit values (2.32) have been taken without changes from Ref. 46. Although V_{NI} is only of minor importance for our results, the influence of all ten parameters on the results has been checked, and will be discussed in Sect. III.

C. Experimental Data

The evaluation of Eqs. (2.6) - (2.9) requires the following input data: the yield and charge assignment of each mass split, the experimental fragment excitation energies (from neutron and γ emission data), and the measured mean kinetic energies per fragment pair.

For the mass yields Y we have taken the pre-neutron emission data of Schmitt, et al.,[50] and for comparison, the earlier data measured by Whetstone.[51]

The fission modes (N_1,Z_1) of ^{252}Cf have been taken from Schmitt's table[28] of energetically favored doubly even fission modes. We take these fission modes even for the high yield mass splits, where experimental mean fragment charges are known, because the discrepancies are small,[28] and additional pairing corrections for the non-integer experimental mean values can be avoided. For the most asymmetric fragment pairs (A_1 = 90, 92) no charge values are given by Schmitt. Here the charge assignment was made after the Myers-Swiatecki mass formula.[40] (It leads to the same fission modes[28] as the Wing-Fong mass formula[52] used by Schmitt.)

The experimental fragment excitation energy E^*_{expt} has been determined according to the relation

$$E^*_{expt}(A_F) = (\bar{B} + \bar{\eta} + 0.75 \text{ MeV})\bar{\nu}(A_F) + 2 \text{ MeV} \tag{2.33}$$

given by Nifenecker, et al.[17] Here $\bar{\nu}$ denotes the measured number of neutrons per fragment, and $\bar{B}$ and $\bar{\eta}$ the average binding and center-of-mass energy per neutron. The other terms account for the energy of the γ quanta.[17,53] The quantity $\bar{B} + \bar{\eta}$ + 0.75 MeV is given in Ref. 17. For the neutron number $\bar{\nu}(A_F)$ we have used the measurements of the Saclay group[17,54,55] and, for comparison, those of Gavron and Fraenkel.[56] For the most symmetric mass splits (A_H = 126, 128, 130) there is a considerable discrepancy between the values resulting from Eq. (2.33) and those following from the Q-value[40] and the fragment kinetic energy.[50] This has been corrected for. In order to test the accuracy of the results we have also used the excitation energies given by Bowman, et al.,[57,58] which are independent of Eq. (2.33).

The experimental kinetic energies per fragment pair E^{kin}_{expt} are taken from Fig. 10 of Schmitt, et al.[50] They are adjusted such that the mean value 186.5 MeV of Ref. 50 is reproduced. In order to estimate the uncertainties entering into our calculation from these data, we have also used values of Whetstone[51] (with a mean value of 185.7 MeV). A discussion of these errors is given in the following section.

III. RESULTS

A. Excitation Energy

The concept of a scission "point" or "line" in the parameter space is defined only within the sharp-surface liquid-drop model with discontinuous break-up of the droplet into two fragments. Actually the nuclear surface has

a certain diffuseness and scission is associated with the formation of a neck with increasing length and decreasing density. Therefore, in the present paper we do not rely on the scission-point concept but study the continuous separation of the fragments by evaluating Eqs. (2.6) - (2.8) separately for a sequence of increasing distances $d = 0,\ldots,\infty$ between the equivalent sharp surfaces of the fragments.[59]

The maximization procedure of Eqs. (2.6) - (2.8) is performed separately for each value of d and for each of 19 pairs of fragments, for which the experimental input data of Subsect. II.C are available. Figure 2 shows the resulting upper bound X_{max} of collective nontranslational plus internal excitation energy of the system as a function of the heavy (H) and light (L) fragment mass for a number of separations d. Here we have allowed X_{max} to vary independently from one fragment pair to the other. The results show that X_{max} is roughly constant[60] for all fragment pairs at a given separation d.

Figure 3 shows the average value $\bar{X}_{max}$ weighted over all 19 mass splits with the yields Y

$$\bar{X}_{max} = \sum_{i=1}^{19} Y_i \, X_{max}(i) / \sum_{i=1}^{19} Y_i . \qquad (3.1)$$

With increasing separation d the resulting value of $\bar{X}_{max}$ increases monotonically up to the experimental fragment excitation energy at a separation of d = 5.3 fm. The increase in $\bar{X}_{max}$ is associated with decreasing deformation energy of the fragments, and a corresponding decrease in fragment deformation.

Even if we disregard very small separations d, where spheroidal fragment shapes may be unrealistic, Fig. 3 indicates rather low dissipation. At d = 1 fm, for instance (where less than 1% of the total mass is contained in the overlap region), the upper bound is $\bar{X}_{max}$ = 7 MeV. Taking this as face value means that in passing through the (d = 1 fm) configuration less than 20% of the experimental

total fragment excitation energy is available for internal and other nontranslational excitation. The internal excitation energy alone should even be smaller.

B. Accuracy

Uncertainties enter into our calculation from both the experimental data and the calculated potential energy. The accuracy of the results of Subsect. II.A has been examined by repeating the calculation with the following modifications:

(i) The unusually large radius parameter $r_c = 1.2249$ fm of the Myers-Swiatecki mass formula[41] has been replaced by $r_c = 1.1$ fm, which is closer to electron scattering data.[62,63]

(ii) The other parameters a_2 and κ of the liquid-drop energy have been changed by 5% and the parameters C and c of the shell energy by 10%. (The accuracy of the original liquid-drop parameter fit[40] is 1-2%.)

(iii) Schematic secondary minima have been included in the deformation energy of each fragment by adding an additional term that is 4 MeV deep, centered at an axis ratio of 2:1, and is a quadratic function of the semi-axis z of the fragment, i.e.,

$$4\ \text{MeV}\left[\left(\frac{z}{r_c A^{1/3}} - 1.6\right)^2 / 0.15^2 - 1\right], \quad 1.45 \le \frac{z}{r_c A^{1/3}} \le 1.75. \qquad (3.2)$$

(iv) The nuclear interaction energy V_{NI} after Krappe and Nix,[46] Eq. (2.27), has been replaced by that of Bass,[47-49] and

(v) has been discarded at all, $V_{NI} = 0$.

(vi) The kinetic energy data E^{kin}_{expt} of Whetstone[51] have been used instead of those of Schmitt, et al.[50]

(vii) The same replacement has been made for the yields Y, which enter into Eq. (3.1).

(viii) The fragment excitation energies E^{*}_{expt} of Eq. (2.33) have been re-evaluated using neutron data of Gavron and Fraenkel,[56]

(ix) and have been replaced by the excitation energies of Bowman, et al.[57]

It turned out that none of the above modifications changes the value of $\bar{I}_{max} = 7$ MeV by more than 50%. Thus an upper bound of 10 MeV for the dissipated plus nontranslational collective excitation energy in ^{252}Cf(sf) should be rather firm within the framework of the spheroidal potential energy and the experimental data of Subsects. II.B and II.C.

Changes in X_{max} that would result from taking another (non-spheroidal) shape parametrization, of course, cannot be predicted in advance. Inclusion of additional parameters (like P_3 deformations or the polarization of the fragment charge densities) would certainly tend to increase X_{max}, since it would increase the parameter space of the minimization procedure. Such calculations would be rather time-consuming as the spheroidal computation scans already about $19 \times 50 \times 50 \times 10 \approx 500{,}000$ points in the $(A_1, \beta_1, \beta_2, d)$ parameter space.

High dissipation, however (up to $X_{max} = E^{*}_{expt}$), is compatible with experiment only if strange nuclear shapes are assumed. In the symmetric fission of ^{252}Cf, for instance, the hypothetical shape of Fig. 4 is required in order to simultaneously satisfy Eq. (2.7) and $X_{max} = E^{*}_{expt}$ (even if $\delta = 0$ and zero deformation energy of the neck is assumed). Shorter necks ($d < 7.4$ fm) do not fit the experimental kinetic energy in Eq. (2.7) unless one allows for distortions of the spheres. Then the fragments have a certain amount of deformation energy, and the dissipation is not complete, $X_{max} < E^{*}_{expt}$.

High dissipation has been obtained in a recent calculation[10] in conjunction with peculiar shapes at scission. It is interesting to note that this is compatible with the results of the present study, which does not rely on the dynamical assumptions made in Ref. 10 (i.e., nearly irrotational hydrodynamics, no shell effects, modified one-body viscosity and the 'rupture' of the neck). However, the fragment excitation energies corresponding to Ref. 10 are not known, and a decision if such peculiar shapes are close to reality or not cannot be made on the basis of the existing fission data.

C. Fragment Deformation

Apart from secondary minima (which are treated below) the potential energy V of Subsect. II.B is a monotonic function of the fragment deformation β

$$V(Z,A,\beta^b) \geq V(Z,A,\beta^a) \quad \text{if } \beta^b > \beta^a \geq \beta^{gst}. \tag{3.3}$$

Therefore, the energy limits of the previous subsections imply certain limits for the deformations of the fragments at the beginning of their separation.

Considering each fragment separately, inequality (2.9) requires that the deformation energy of each fragment (relative to its ground state deformation β^{gst}) is smaller than its experimental excitation energy, i.e.,

$$V(Z,A,\beta) - V(Z,A,\beta^{gst}) \leq E^*_{expt}(Z,A) \tag{3.4}$$

and, according to Eq. (3.3)

$$V(Z,A,\beta) \leq V(Z,A,\beta_{max}) = E^*_{expt}(Z,A) + V(Z,A,\beta^{gst}). \tag{3.5}$$

The upper bounds for the deformations β of the single fragments are given in Fig. 5 as a function of the fragment mass number A_F. The upper bound β_{max} of Eq. (3.5) is independent of d. The figure shows that the heavy fragments around the doubly magic one ($A_H = 132$) have to be almost undeformed if their kinetic and excitation energies are to be compatible with experiment.

In a recent paper Wilkins, et al.,[36] attribute a number of effects in fission to the occurrence of deformed (secondary) shells in some fragments. Our results give no evidence that the fragment deformations are affected by secondary fragments shells. Even the inclusion of an artificial secondary minimum in the potential energy of *each* fragment (by the additional term (3.2)) leaves the results almost unchanged. The negligible influence of secondary fragment shells is in accordance with the earlier results of Dickmann and Dietrich.[30]

D. Minimum Potential Energy Hypothesis

A number of calculations dealing with a nucleus at scission is based on the hypothesis that the deformation at scission is associated with minimum potential energy in a certain parameter space that is restricted to scission-type configurations. The hypothesis is usually advocated by assuming the change in nuclear shape to be slow compared with the motion of the nucleons ("adiabatic assumption") or by taking the scission point to be a stationary point of the potential energy surface ("scission minimum").

In the present work we do not employ the adiabatic assumption nor do our results give evidence for a scission minimum. For comparison, however, we have also considered the deformations and energies that would follow from minimizing the potential energy of the scission configuration, i.e.,

$$\sum_{i=1}^{2} V(Z_i,A_i,\beta_i) + V_{int}(Z_1,Z_2,A_1,A_2,\beta_1,\beta_2,d) = \text{minimum}. \tag{3.6}$$

The deformations $\beta_{\text{min. energy}}$ which follow from the minimum conditions $\partial V/\partial\beta_i + \partial V_{int}/\partial\beta_i = 0$ are almost independent of d because the derivatives $\partial V_{int}/\partial\beta_i$ depend only weakly on d and V is independent of d.

Figure 5 shows these β values calculated after the customary condition of minimum potential energy (3.6). We find that the deformations of minimum energy are outside our bounds for all fragments with mass numbers A_H between 126 and 146. The discrepancy is particularly large for the fragments around the doubly magic one with mass number $A_H = 132$.

We have also plotted the β values of the *local* minimum (if any) in the (β_1,β_2) plane that is caused by the ground-state shell effect of the heavy fragment. This criterion has previously been used by Dickmann and Dietrich[30] (cf. Fig. 3b of Ref. 30). It can be seen that the β values associated with the shell effect in the heavy fragment generally are in agreement with the limit

β_{max}. The local shell minima occur only in fragments with mass numbers A_H between 126 and 138, i.e., in the mass region with the largest discrepancies between the deformations of minimum energy and our bound β_{max}. Therefore, the local shell minimum leads to a spectacular improvement in deformation (cf. Fig. 5). Thus the fragmentation in fission seems to be determined by the doubly shell closure (Z = 50, N = 82) rather than by adiabatic nuclear motion in the vicinity of the scission point.

E. Ternary Fission

In a number of papers (cf. Refs. 64-66 and refs. given therein) the trajectories of long-range alpha particles (LRA) emitted in fission have been studied in order to obtain information about the fissioning nucleus at the beginning of the fragment separation. Although there are large discrepancies between various results of different groups, the agreement is satisfactory for the center-to-center distances D resulting from such calculations (for a compilation of LRA data see Ref. 64, Table XIV-3). Most analyses[64,65] of LRA data yield rather high values of D (around 25 fm).

A comparison with Fig. 6 shows that the LRA values of $D = z_1 + z_2 + d$ are in accord with our fragment deformations only if we assume unreasonably large fragment separations of d = 5 fm or more. We therefore conclude that LRA fission is different from ordinary binary fission (without alpha emission): Either the alpha particles are emitted only in (rare) fission events with particular elongation of the scission configuration or the alpha particles are emitted after scission at some separation (viz. roughly d = 5 fm). Similar discrepancies between binary and ternary fission have been noted earlier by several authors.[9,64,66]

IV. CONCLUSIONS

We have derived general inequalities that relate the nuclear nontranslational excitation energy at (and after) scission to the measured data for fragment kinetic energies, neutron and γ-ray emission. For spheroidal fragment shapes an upper bound of only $\bar{X}_{max} = 7$ MeV is determined for the vibrational plus rotational collective plus internal excitation energy in ^{252}Cf(sf). The uncertainties entering into that value from both the experimental data and the potential energy are found to be less than 50%. According to that the energy available in the spontaneous fission of ^{252}Cf (roughly 50 MeV, see Fig. 3) is at most weakly dissipated. The assumption of high or complete damping can be ruled out unless one allows for unreasonable fragment shapes (like Fig. 4).

Upper bounds have also been obtained for the deformations of the fragments (Fig. 5). The hypothesis of minimum potential energy at scission is found to disagree with our analysis for mass divisions close to the heavy fragment mass $A_H = 132$. On the contrary, a decisive influence on the fragmentation from the double shell closure (Z = 50, N = 82) in the heavy fragment is in accord with our results. We find no evidence for effects from secondary fragment shells.[36]

The authors are grateful to Drs. R. Bass, F. Dickmann, F. Gönnenwein, J. J. Griffin, P. C. Lichtner and A. B. Volkov for helpful discussions and correspondence.

REFERENCES

Work supported by the German Bundesministerium für Forschung und Technologie, the Deutsche Forschungsgemeinschaft, the U. S. Department of Energy and the University of Maryland Computer Science Center.

1. D. L. Hill and J. A. Wheeler, Phys. Rev. 89, 1102 (1953).
2. J. R. Nix, University of California Lawrence Radiation Laboratory Report No. UCRL-11338, 1964 (unpublished).
3. J. R. Nix and W. J. Swiatecki, Nucl. Phys. 71, 1 (1965).
4. J. R. Nix, Nucl. Phys. A130, 241 (1969).
5. R. W. Hasse, Phys. Lett. 27B, 605 (1968); Nucl. Phys. A128, 609 (1969); Phys. Rev. C4, 572 (1971).
6. P. Fong, Proc. 2nd IAEA Symp. on physics and chemistry of fission, Vienna, 1969 (IAEA Vienna, 1969), p. 133; Statistical theory of nuclear fission (Gordon and Breach, New York, 1969).
7. R. Wieczorek, R. W. Hasse and G. Süssmann, Proc. 3rd IAEA Symp. on physics and chemistry of fission, Rochester, 1973 (IAEA, Vienna, 1974), Vol. 1, p. 523.
   R. W. Hasse, Nuclear friction, preprint [University of Munich, 1977 (unpublished)].
8. J. R. Nix and A. J. Sierk, Physica Scripta 10A, 94 (1974).
9. K. T. R. Davies, A. J. Sierk and J. R. Nix, Phys. Rev. C13, 2385 (1976).
10. A. J. Sierk, S. E. Koonin and J. R. Nix, Phys. Rev. C17, 646 (1978).
11. W. J. Swiatecki, Proc. Intl. School-Seminar on reactions of heavy ions with nuclei and synthesis of new elements, Dubna, USSR, 1975 [Joint Inst. for Nuclear Research Report No. JINR-D7-9734, 1976 (unpublished)]. p. 89.
12. J. Błocki, Y. Boneh, J. R. Nix, J. Randrup, M. Robel, A. J. Sierk, and W. J. Swiatecki, Lawrence Berkeley Laboratory Report No. LBL-6536, 1977 (unpublished).

13. Y. Boneh, J. Błocki and W. D. Myers, Proc. 4th Intl. Workshop on gross properties of nuclei and nuclear excitations, Hirschegg, Austria, 1976 [Technische Hochschule Darmstadt Report No. AED-Conf-76-015-000, 1976 (unpublished)], p. 77; Phys. Lett. 63B, 265 (1976).
14. W. J. Swiatecki, Proc. Intl. Conf. on nuclear reactions induced by heavy ions, Heidelberg, 1969, ed. R. Bock and W. R. Hering (North-Holland, Amsterdam-London, 1970), p. 729; J. Physique Suppl. 33, C5-45 (1972).
15. S. Bjørnholm, Proc. 5th Summer School on nuclear physics, Rudziska, Poland, 1972, ed. E. Cieslak, M. Dabrowska and A. Saganek [Inst. of Nuclear Research Report No. INR-P-1447/I/PL, Warsaw, 1972 (unpublished)], Vol. 1, p. 131; Physica Scripta 10A, 110 (1974).
16. W. J. Swiatecki and S. Bjørnholm, Phys. Rep. 4, 325 (1972).
17. H. Nifenecker, C. Signarbieux, R. Babinet, and J. Poitou, Proc. 3rd IAEA Symp. on physics and chemistry of fission, Rochester, 1973 (IAEA, Vienna, 1974), Vol. 2, p. 117.
18. H. Schultheis and R. Schultheis, Phys. Lett. 57B, 7 (1975).
19. P. Armbruster, Proc. 3rd Intl. Workshop on gross properties of nuclei and nuclear excitations, Hirschegg, Austria, 1975 [Technische Hochschule Darmstadt Report No. AED-Conf-75-009-000, 1975 (unpublished)], p. 32.
20. A. Michaudon, Proc. Intl. Conf. on the interactions of neutrons with nuclei, Lowell, Mass., 1976, ed. E. Sheldon (Technical Information Center, Energy Research and Development Administration, CONF-760715-P1, Springfield, Virginia, 1976), Vol. 1, p. 641.
21. L. Wilets, Theories of nuclear fission (Clarendon Press, Oxford, 1964).
22. G. Schütte and L. Wilets, Proc. 3rd IAEA Symp. on physics and chemistry of fission, Rochester, 1973 (IAEA, Vienna, 1974), Vol. 1, p. 503; Nucl. Phys. A252, 21 (1975).

23. Y. Boneh and Z. Fraenkel, Phys. Rev. C10, 893 (1974).

24. K. T. R. Davies, S. E. Koonin, J. R. Nix and A. J. Sierk, Proc. 3rd Intl. Workshop on gross properties of nuclei and nuclear excitations, Hirschegg, Austria, 1975 [Technische Hochschule Darmstadt Report No. AED-Conf-75-009-000, 1975 (unpublished)], p. 8.

25. S. E. Koonin and J. R. Nix, Phys. Rev. C13, 209 (1976).

26. R. Vandenbosch, Nucl. Phys. 46, 129 (1963).

27. V. S. Stavinsky and L. N. Shehata, Nucl. Phys. 62, 145 (1965).

28. H. W. Schmitt, Ark. Fys. 35, 633 (1967).

29. A. V. Ignatyuk, Sov. J. Nucl. Phys. 7, 626 (1968).

30. F. Dickmann and K. Dietrich, Nucl. Phys. A129, 241 (1969).

31. V. A. Rubchenya, Sov. J. Nucl. Phys. 9, 697 (1969).

32. P. Armbruster, Nucl. Phys. A140, 385 (1970).

33. B. D. Wilkins and E. P. Steinberg, Phys. Lett. 42B, 141 (1972).

34. B. D. Wilkins, E. P. Steinberg and R. R. Chasman, Proc. 3rd IAEA Symp. on physics and chemistry of fission, Rochester, 1973 (IAEA, Vienna, 1974), Vol. 2, p. 496.

35. H. Schultheis and R. Schultheis, Nuovo Cim. Lett. 6, 159 (1973); Nucl. Phys. A215, 329 (1973); Nukleonika 19, 645 (1974); Phys. Lett. 52B, 389 (1974); J. Math. Phys. 16, 905 (1975).

36. B. D. Wilkins, E. P. Steinberg and R. R. Chasman, Phys. Rev. C14, 1832 (1976).

37. P. Armbruster, Proc. 1st IAEA Symp. on physics and chemistry of fission, Salzburg, 1965 (IAEA, Vienna, 1965), Vol. 1, p. 103.

38. W. Nörenberg, Z. Phys. 197, 246 (1966); Phys. Rev. C5, 2020 (1972).

39. A. Bohr and B. R. Mottelson, Mat. Fys. Medd. Dan. Vid. Selsk. 27 (1953), No. 16.

40. W. D. Myers and W. J. Swiatecki, Nucl. Phys. 81, 1 (1966).

41. W. D. Myers and W. J. Swiatecki, Ark. Fys. 36, 343 (1967).

42. S. Flügge, Z. Phys. 130, 159 (1951).

43. A. J. Sierk and J. R. Nix, Los Alamos Scientific Laboratory Report No. LAP-151, 1976 (unpublished).

44. B. C. Carlson, J. Math. Phys. 2, 441 (1961).

45. W. Scheid and W. Greiner, Z. Phys. 226, 364 (1969).

46. H. J. Krappe and J. R. Nix, Proc. 3rd IAEA Symp. on physics and chemistry of fission, Rochester, 1973 (IAEA, Vienna, 1974), Vol. 1, p. 159; H. J. Krappe, Proc. MPI Heidelberg Symp. on classical and quantum mechanical aspects of heavy ion collisions, Heidelberg, 1974, ed. H. L. Harney, P. Braun-Munzinger and C. K. Gelbke (Springer, Berlin-Heidelberg-New York, 1975), p. 24.

47. R. Bass, Phys. Lett. 47B, 139 (1973); Nucl. Phys. A231, 45 (1974).

48. R. Bass, private communication.

49. The recent modification (R. Bass, Phys. Rev. Lett. 39, 265 (1977)) has not been used in the present work.

50. H. W. Schmitt, J. H. Neiler and F. J. Walter, Phys. Rev. 141, 1146 (1966).

51. S. L. Whetstone, Phys. Rev. 131, 123 (1963).

52. J. Wing and P. Fong, Phys. Rev. 136, B923 (1964).

53. H. Nifenecker, C. Signarbieux, M. Ribrag, J. Poitou and J. Matuszek, Nucl. Phys. A189, 285 (1972).

54. C. Signarbieux, J. Poitou, M. Ribrag and J. Matuszek, Phys. Lett. 39B, 503 (1972).

55. C. Signarbieux, H. Nifenecker, J. Poitou and M. Ribrag, J. Physique Suppl. 33, II-25 (1972).

56. A. Gavron and Z. Fraenkel, Phys. Rev. C9, 632 (1974).

57. H. R. Bowman, J. C. D. Milton, S. G. Thompson and W. J. Swiatecki, Phys. Rev. 129, 2133 (1963).

58. After completion of our calculation new data (R. L. Walsh and J. W. Boldeman, Nucl. Phys. A276, 189 (1977)) have been published, which are closer to those of Ref. 57.

59. The variable d (the distance between the equivalent sharp surfaces of the fragments) should not be confused with the neck parameter of sharp-surface calculations (e.g., our previous estimate, Ref. 18). The latter is no degree of freedom but a correction to the sharp-surface Coulomb repulsion energy at the scission point.

60. The assumption of a constant ratio X_{max}/E^*_{expt} of our previous calculation[18] is not well fulfilled for the fragment pairs close to symmetry. However, due to the low yields in these cases the resulting average $\bar{X}_{max}$ is not much affected.

61. J. N. P. Lawrence, Phys. Rev. 139, B1227 (1965).

62. L. R. B. Elton, Nuclear sizes (Oxford University Press, Oxford, 1961).

63. R. Hofstadter, Rev. Mod. Phys. 28, 214 (1956); Ann. Rev. Nucl. Sci. 7, 231 (1957).

64. R. Vandenbosch and J. R. Huizenga, Nuclear fission (Academic Press, New York, London, 1973).

65. F. Fossati and T. Pinelli, Nucl. Phys. A249, 185 (1975).

66. A. Gavron, Phys. Rev. C11, 580 (1975).

FIGURE CAPTIONS

Fig. 1: Simplified example for the evaluation of Eqs. (2.6) - (2.9) in the case of symmetric fission with only one deformation parameter β. The solid lines show the fragment deformation energy (Fig. 1a) and the Coulomb repulsion between the fragments as (calculated) functions of the fragment deformation β. The horizontal dashed lines give the experimental values. The quantities resulting from the procedure described in the text are the upper bound X_{max} for internal excitation and the upper bound β_{max} for the fragment deformation.

Fig. 2: Calculated upper bounds X_{max} of the internal plus nontranslational collective excitation energy per fragment pair at a number of separations d. Experimental data for E^*_{expt} are taken from Refs. 17, 54, 55 (cf. Subsect. II.C).

Fig. 3: Calculated upper bound for the internal plus nontranslational collective excitation energy in ^{252}Cf(sf) as a function of the separation d between the equivalent sharp density surfaces of the fragments. The experimental mean fragment excitation energy $\overline{E^*_{expt}}$ is determined after Refs. 17, 50, 54, 55 as described in Subsect. II.C. For comparison the figure also shows the maximum (static) liquid drop energy[41] release at scission (here taken to be the energy of the lowest point on the scission line of Lawrence's shape parametrization[61] relative to its ground state).

Fig. 4: Hypothetical nuclear shape required to make total dissipation $X_{max} \approx E^*_{expt}$ compatible with the experimental ^{252}Cf symmetric fission data (here shell effects are neglected). Complete dissipation can be ruled out for shorter necks or distorted fragments as used in the present work.

Fig. 5: Calculated fragment deformation β at scission as a function of the fragment mass number A_F. The curve labelled "min. energy" is determined from Eq. (3.6). The label shell minimum refers to the local potential energy minimum that is caused by the ground-state shell effect in the heavy fragment. The quantity β_{max} is independent of d, and $\beta_{min.\ energy}$ is rather insensitive to d, as discussed in the text.

Fig. 6: Upper bounds for the lengths of the semi-axes $z_1 + z_2$ of the fragments. The values are calculated from β_{max} of Fig. 5 according to Eq. (2.11).

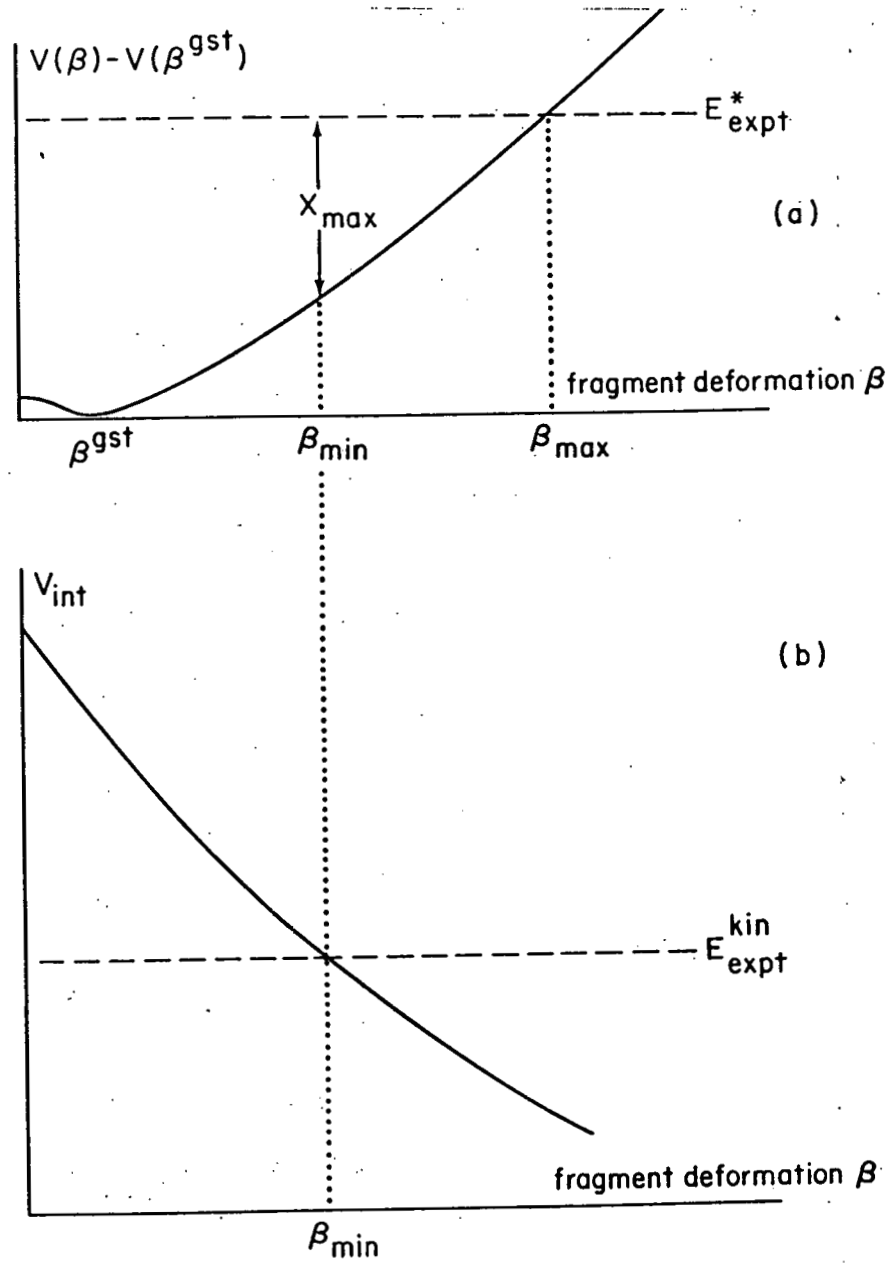

Fig. 1

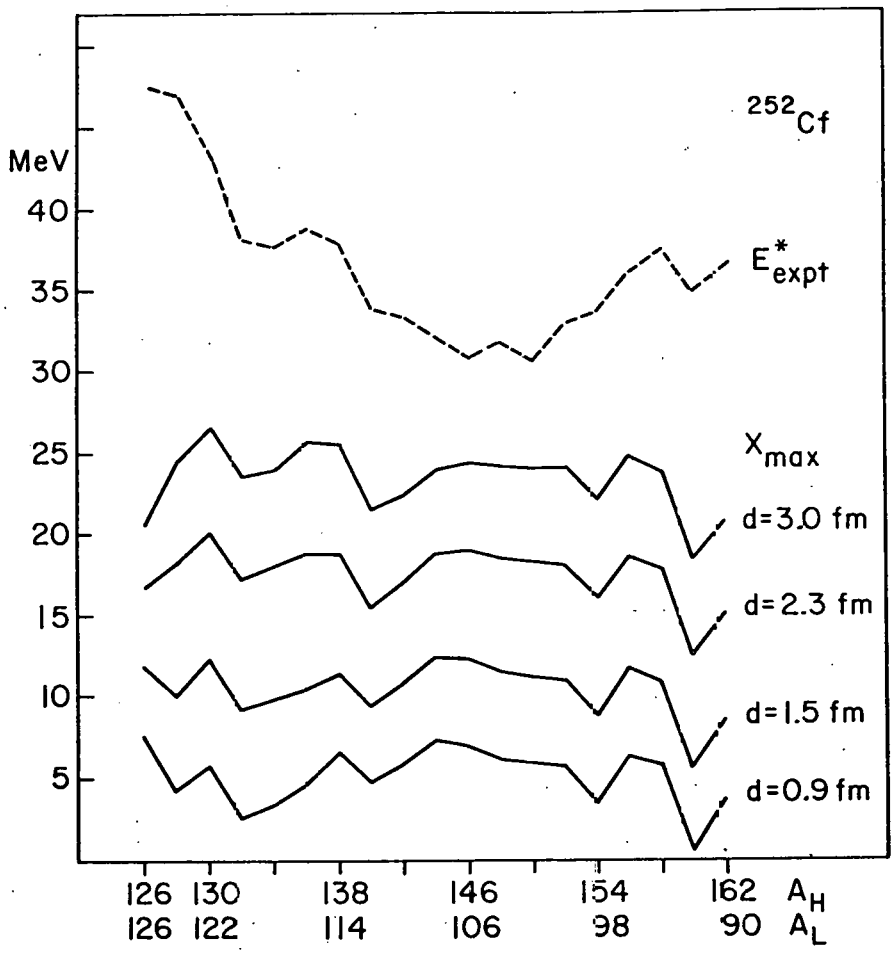
MeV
40
35
30
25
20
15
10
5
^{252}Cf
E^*_{expt}
X_{max}
d=3.0 fm
d=2.3 fm
d=1.5 fm
d=0.9 fm
126 130 138 146 154 162 A_H
126 122 114 106 98 90 A_L

Fig. 2

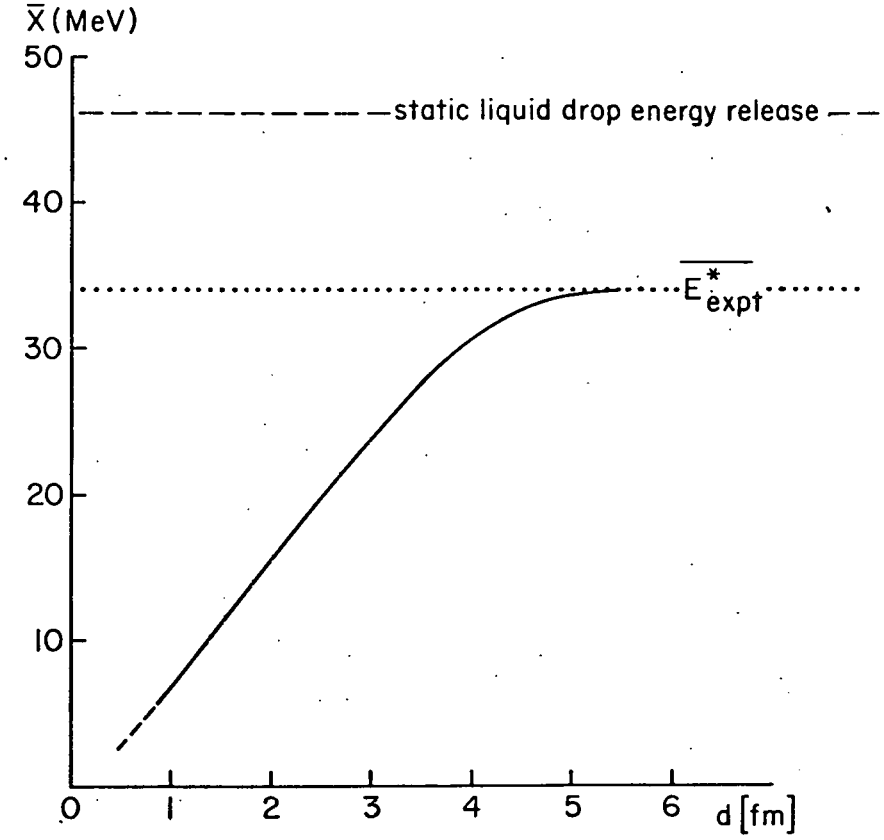
$\bar{X}$(MeV)
50
40
30
20
10
static liquid drop energy release
$\overline{E^*_{expt}}$
0 1 2 3 4 5 6 d[fm]

Fig. 3

Fig. 4

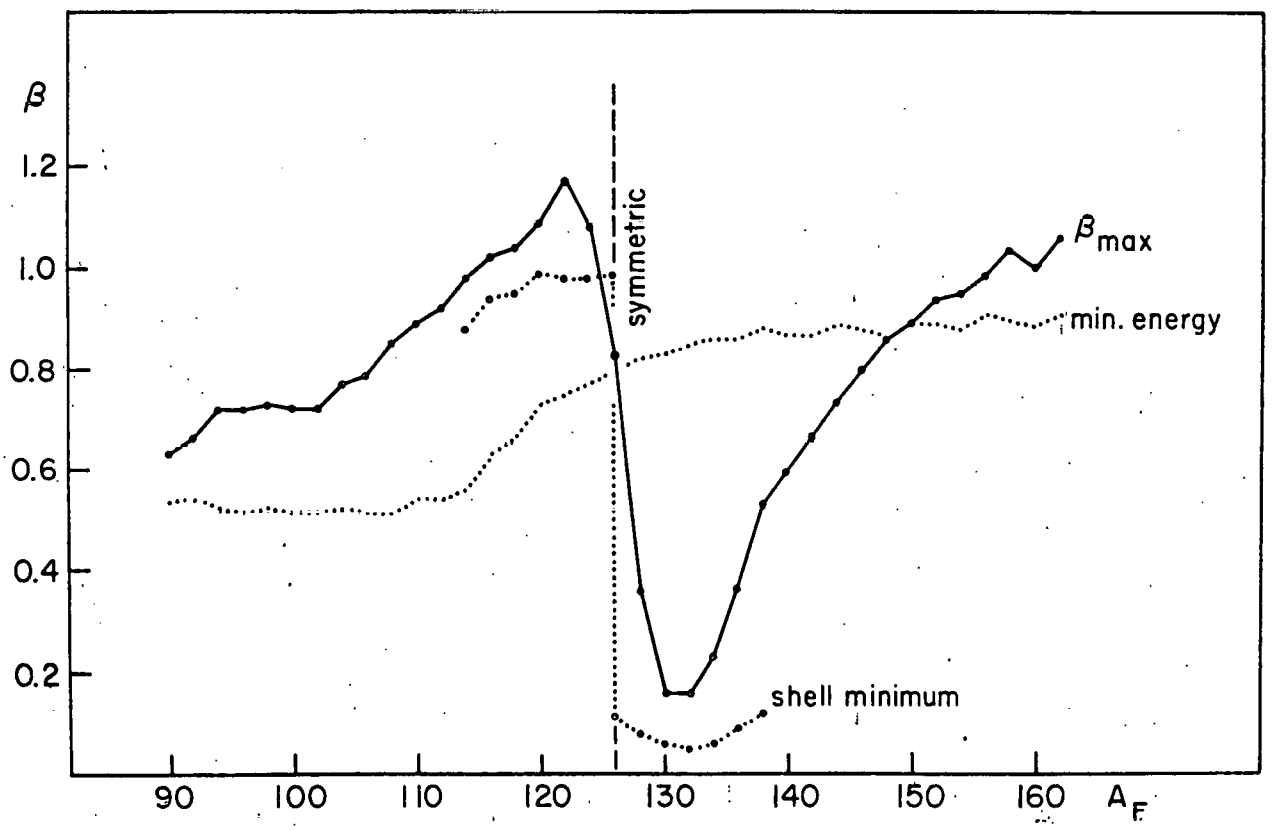
β
1.2
1.0
0.8
0.6
0.4
0.2
symmetric
β_{max}
min. energy
shell minimum
90
100
110
120
130
140
150
160
A_F

Fig. 5

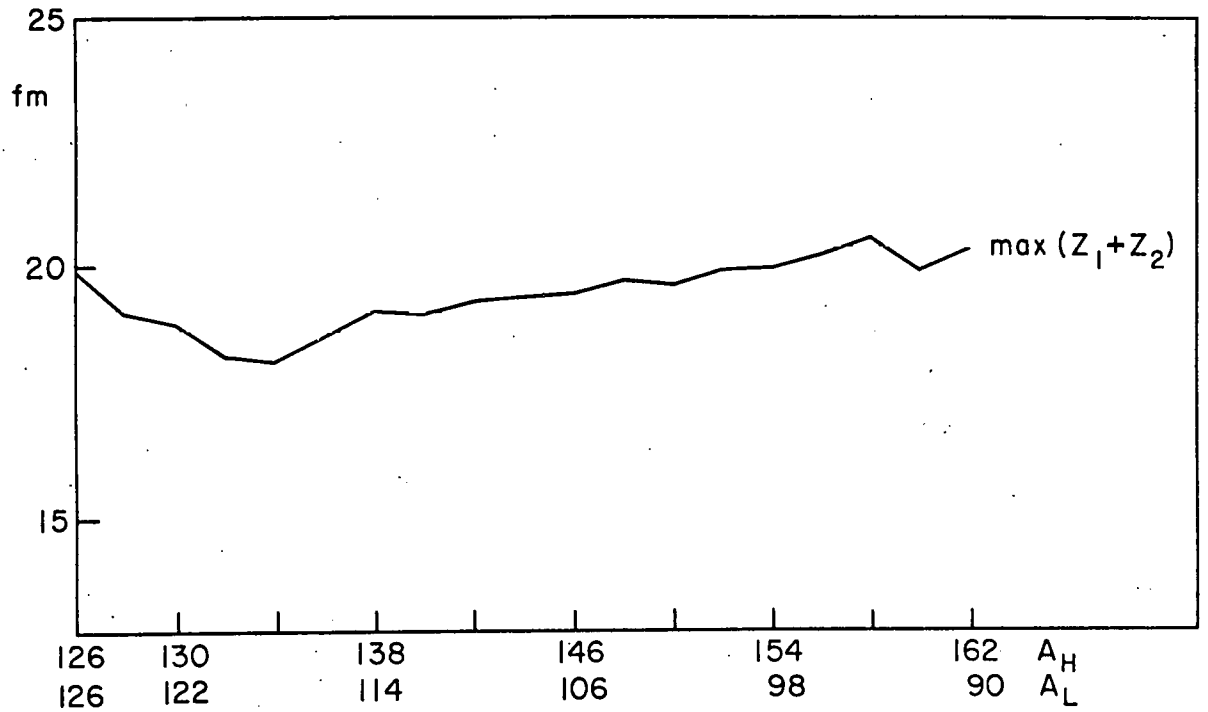
25
fm
20
15
max (Z_1+Z_2)
126 130 138 146 154 162 A_H
126 122 114 106 98 90 A_L

Fig. 6